BULETINUL INSTITUTULUI POLITEHNIC DIN IAŞI
Publicat de
Universitatea Tehnică „Gheorghe Asachi” din Iaşi
Volumul 69 (73), Numărul 2, 2023
Secţia
ELECTROTEHNICĂ. ENERGETICĂ. ELECTRONICĂ
DOI:10.2478/bipie-2023-0007

COMPARISON OF LINEAR QUADRATIC REGULATOR AND MODEL PREDICTIVE CONTROL BASED ALGORITHMS IN CONTINUOUS PRODUCTION

BY

AMELIA CHINDRUŞ[1,*], DANA COPOŢ[2] and CONSTANTIN-FLORIN CĂRUNTU[1]

[1]“Gheorghe Asachi” Technical University of Iași, Romania,
Faculty of Automatic Control and Computer Engineering
[2]Ghent University of Ghent, Belgium,
Faculty of Engineering and Architecture

Received: February 10, 2023
Accepted for publication: June 3, 2024

Abstract. The integration of Industry 4.0 into manufacturing processes necessitates the automation of complex, large-scale operations within cyber-physical systems (CPSs). Pharmaceutical manufacturing, in particular, requires a transition from traditional batch processing to continuous manufacturing to achieve seamless integration with CPSs. This paper explores the comparison between two control strategies for pharmaceutical tablet production: the linear quadratic regulator (LQR) method and an established model predictive control (MPC) algorithm. The LQR method focuses on providing optimal stability and robustness for the plant's operations, particularly through centralized management of key process units in the dry granulation process. A detailed plant model is utilized to test the performance of the LQR controller, with results benchmarked against those obtained using the MPC algorithm.

*Corresponding author; *e-mail*: amelia.vatamanu@student.tuiasi.ro

Keywords: Cyber-physical system, continuous manufacturing, Industry 4.0, linear quadratic regulator, model predictive control.

1. Introduction

The rapid development of new technologies and rising consumer demands are driving the need for increased flexibility and production quality across all industries. This pressure has driven to the emergence of Cyber-Physical Systems (CPSs) within the framework of the Fourth Industrial Revolution, also known as Industry 4.0. CPSs involve large-scale networks of diverse components that integrate computational capabilities with physical processes through data exchanges, enabling intelligent monitoring and control of various environments.

Cyber-Physical Systems bridge physical operations with advanced computing and communication infrastructures (Jazdi, 2014). The physical component includes the actual processes and physical objects, such as sensors, actuators, and equipment, used for monitoring, coordinating and controlling activities. The cyber component is divided into two layers: the first layer is responsible for activating and ensuring the proper operation of the physical components, while the second layer manages the computational processes that control the physical operations based on implemented logic and operational domains. CPSs are being integrated into various fields, including transportation systems (Deka *et al.*, 2018), the Industrial Internet of Things (IIoT) (Tao *et al.*, 2018), healthcare medical system (Dey *et al.*, 2018), smart home (Do *et al.*, 2018) and energy systems (Jha *et al.*, 2021). These systems support the digitalization and automation of processes, improving the efficiency, reliability and overall performance of industrial operations.

For example, Senior Software company proposes the implementation of a complete production management system (MES – Manufacturing Execution System), customized according to the field of activity, which guarantees control over all operations in the factory, from the moment when the order is received from the customer to the final product. They claim that companies that have already implemented this system have achieved a 20% increase in productivity, a 45% reduction in production cycle time, an 18% reduction in manufacturing defects, and a 75% reduction in data entry time.

To integrate cyber-physical systems into a manufacturing plant and adapt production to new technologies, it is essential, primarily, to automate manufacturing processes. Thus, continuous manufacturing (CM) is a starting point in this direction, with the aim of increasing production flexibility, lead times and costs, and reducing human errors that can affect the quality of finished products. Continuous manufacturing involves producing products and processing materials without interruption. Continuous processes became

popular in the early 20th century, but the first continuous-flow processes were patented as early as 1799 with the introduction of the first Fourdrinier paper machine (Haunreiter, 1997), which produced a roll of paper, starting with the raw material and following specific steps.

In the pharmaceutical industry, oral tablet production predominantly utilizes batch manufacturing. However, there are significant differences between batch and continuous manufacturing processes. The table below illustrates some of these comparative characteristics. Continuous manufacturing, unlike batch processing, requires time for startup and shutdown and is subject to dynamic disturbances. Consequently, continuous manufacturing systems integrate both feedback and feedforward control mechanisms to address real-time disturbances across various production units. Continuous manufacturing in pharmaceuticals requires sophisticated control techniques to maintain uniform product quality and operational efficiency. The integration of feedback control allows the system to correct deviations by comparing actual outputs to desired set points, while feedforward control anticipates and compensates for disturbances before they affect the process. This dual-control approach is crucial for maintaining the stability and robustness of continuous production systems in the face of inherent dynamic disturbances.

Table 1

Characteristics of batch and continuous production

	Batch manufacturing	**Continuous production**
Raw material input/ Product output	Raw materials are added to the process in batches and the product is released all at once after the process is completed.	Raw materials are fed continuously into the process and the product is released steadily over time.
Production processes	Operations start and stop frequently, requiring operator intervention for each batch.	Operations run continuously, with interconnected units and automation, requiring minimal operator intervention.
Production facility area	Requires a large facility space due to the start-stop nature of batch processes.	More space-efficient due to continuous, streamlined operations.
Scaling-up	Scaling up requires separate validation and specialized equipment for each production stage, with different setups for commercial production.	Scaling up is more straightforward, as development equipment can be designed to match production needs, enabling a seamless transition to full-scale production by adjusting time parameters.

The main goal of any manufacturer is to maximize profit, so, CM is a sure way to reduce production costs by reducing waste when defects are detected, wage costs and production time. Additionally, CM offers the critical advantage of increased production volumes, which is essential to meet the rising demand for products and services that enhance the quality of life.

The manufacturing process for oral solid dosage forms in the pharmaceutical industry comprises several critical steps. These steps include powder feeding, blending, milling, granulation, tableting and coating (Sen *et al.*, 2012). On advances in tablet manufacturing process control, recent studies have approached methods such as Proportional-Integral-Derivative (PID) control (Malevez and Copoț, 2021), Model Predictive Control (MPC) (Jelsch *et al.*, 2021) or hybrid MPC-PID strategies (Haas *et al.*, 2017).

This study presents a Linear Quadratic Regulator (LQR) control algorithm with integral action for a dry granulation tablet manufacturing process. It compares the performance of this control approach to that of a previously established predictive control method (Copoț *et al.*, 2022), using the same plant model. The LQR control strategy is designed to simultaneously manage all operational units within the manufacturing process. To implement effective control, a Luenberger observer is employed to estimate the system states that are not directly measurable. Simulation results demonstrate that the proposed LQR control strategy successfully maintains system outputs within the specified constraints, even when reference inputs change. This indicates the potential for robust and stable control in complex pharmaceutical manufacturing environments.

2. Process model

In the pharmaceutical industry, there is a growing need to embrace the concept of Cyber-Physical Systems to revolutionize manufacturing processes. Currently, pharmaceutical manufacturing predominantly relies on batch production methods, where materials are stored and processed sequentially, with quality testing conducted offline (Lee *et al.*, 2015). In contrast, continuous manufacturing involves the direct transfer of products between processing units, eliminating the need for intermediate storage. This shift necessitates the development of sophisticated control strategies to ensure stringent quality standards and precise process control, ultimately leading to enhanced productivity and reduced production times. Unlike batch production, continuous manufacturing follows a flow production approach, allowing for uninterrupted process flow without breaks between production steps.

In the pre-distribution phase, oral solid dosage forms undergo rigorous quality assessments, including tests for active ingredient content, weight uniformity, dissolution behavior and mechanical strength. Common challenges encountered during tablet compression processes include variations in weight,

inadequate mechanical strength, poor mixing and tablet layer separation (Bhowmik *et al.*, 2014).

The manufacturing of solid oral tablets primarily involves three main processes: wet granulation, direct compression and dry granulation. Fig. 1 illustrates the continuous manufacturing routes for wet granulation (highlighted in red) and direct compression (indicated in green).

This research specifically focuses on the dry granulation process of solid tablets, which is simulated using Simulink. The process model is constructed based on numerical data extracted from existing literature sources. Key components of the model include feeders for active pharmaceutical ingredients (APIs) and excipients, a blending unit, and hoppers connected to the roller compactor (RC) and tablet press (TP) (Chindruș *et al.*, 2023). Fig. 2 outlines the sequential production steps and the interdependencies between various processing units.

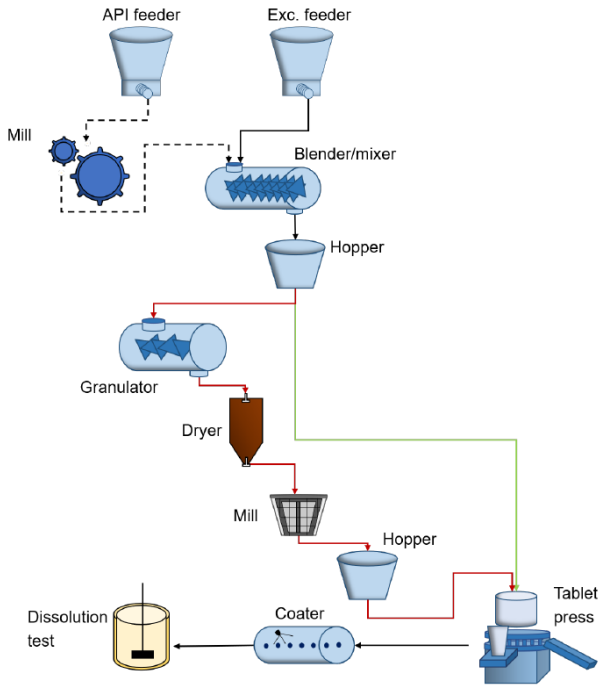

Fig. 1 – Wet granulation (shown in red) and direct compaction (shown in green) used in continuous pharmaceutical tablet manufacturing processes (Chindruș *et al.*, 2023).

The primary goal of the feeding unit operation is to ensure a consistent supply of API, excipients and lubricants to the subsequent unit. This is done while maintaining a steady flow rate to align with the required mixture composition and overall material flow rate. In continuous processes, the screw

feeder emerges as the most prevalent choice. It comprises a feed hopper, one or more bridge-breaking systems and either a single or twin configuration of conveying screws. These components work together to distribute materials out of the unit efficiently (Yu, 1997). One of the major advantages of using screw feeders is their capability to handle extremely low flow rates with precision, ensuring accurate delivery. Within this operation, a crucial parameter to consider is the feed factor. This term refers to the quantity of powder contained in one screw pitch per rotation of the feed screw. The calculation of the feed factor is essential for optimizing the feeding process and maintaining consistent material distribution:

$$ff = \frac{\dot{m}}{\omega}, \tag{1}$$

where $\dot{m}$ is the mass flow rate and ω is the screw speed. According to Heckel's equation, (Escotet Espinoza, 2018; Wang *et al.*, 2017) designed and tested a feed factor model as follows:

$$ff_{aparent}(W) = ff_{\max} - (ff_{\max} - ff_{\min})e^{-\beta W}. \tag{2}$$

Here, W represents the weight of the material inside the feeder, $ff_{\max}$ denotes the maximum relative bulk density within the screws and $ff_{\min}$ indicates the minimum relative bulk density or powder compressibility within the screws (Chindruș *et al.*, 2023). The constant parameter β within the exponential in the above equation represents the rate at which the amount of powder present in the screw pitch decreases concerning the decrease in feeder weight (Bhalode and Ierapetritou, 2020). This is mathematically expressed as:

$$\beta = \frac{Kg}{A_{feeder}}, \tag{3}$$

where K represents the changed pressure decrease constant, g represents the acceleration due to gravity and A_{feeder} denotes the cross-sectional area of the feeder.

The development of a mathematical model for continuous blending relies on the population equation (Sen *et al.*, 2012) as follows in Eq. (4), where F represents the population distribution function, x is the vector of internal coordinates representing particle size and t denotes time. R_{form} and R_{dep} indicate the particles formed and depleted, while $\dot{F}_{in}$ and $\dot{F}_{out}$ denote the rates at which components are fed into or neglected from the system.

$$\frac{\partial F(x,t)}{\partial t} + \frac{\partial}{\partial x}\left(F(x,t)\frac{\partial x}{\partial t}\right) = R_{form}(x,t) - R_{dep}(x,t) + \dot{F}_{in}(x,t) - \dot{F}_{out}(x,t) \tag{4}$$

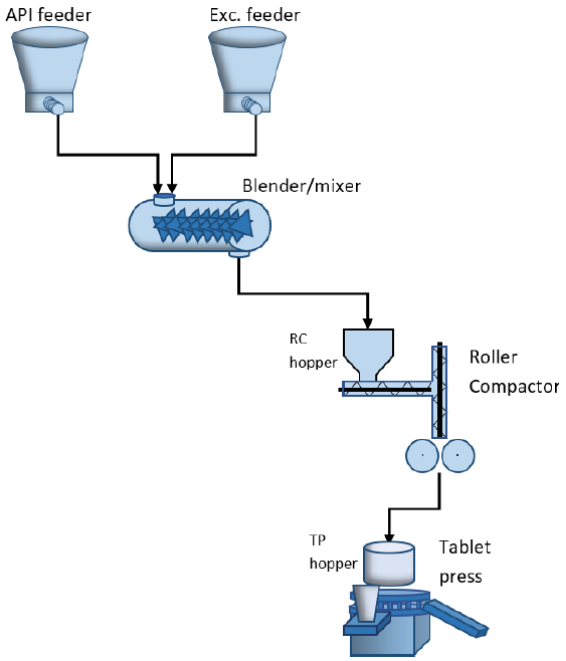

Fig. 2 – Pilot plant for continuous pharmaceutical manufacturing using dry granulation (Chindruș *et al.*, 2022).

As a result of the increased complexity of the system and the limited number of numerical parameters, the blender is divided into multiple sections. These local uniform compartments result from the discretization of the blend container space both axially and radially (Chindruș *et al.*, 2023). Applying Eq. (4) to this process leads to a straightforward mass balance equation for a compartment holding powder streams:

$$\frac{\partial m_{ij}}{\partial t} = F_f\left[m_{i-1,j} - m_{i,j}\right] + F_b\left[m_{i+1,j} - m_{i,j}\right] + F_r\left[m_{i,j+1} + m_{i,j-1} - m_{i,j}\right], \quad (5)$$

where $m_{i,j}$ is the mass holdup in the compartment. The forward $\left(F_f\right)$, backward $\left(F_b\right)$ and radial $\left(F_r\right)$ fluxes are determined using:

$$\begin{aligned} F_f &= a\omega_{blender} + b, \\ F_b &= c\omega_{blender} + d, \\ F_r &= e, \end{aligned} \quad (6)$$

where $\omega_{blender}$ is the blender's speed. The constant parameters used for forward flow (a,b), for flow flux (c,d) and for radial flow (e) are calculated from experimental data, varying with the material type (API or excipient).

Given the subsequent formulation for the flow at the outlet of the blender:

$$F_{blender} = \sum_{j=1}^{N_r} F_{f,API} m_{API,i=N_a,j} + \sum_{j=1}^{N_r} F_{f,Excipient} m_{Excipient,i=N_a,j} , \tag{7}$$

where m_{API} and $m_{Excipient}$ represent the powder holdups of the final compartments in the axial direction, N_r denotes the number of radial discretization and N_a Na indicates the number of axial compartments, the outlet concentration $\left(C_{API}\right)$ is determined as shown:

$$C_{API} = \frac{\sum_{j=1}^{N_r} F_{f,API} m_{API,i=N_a,j}}{F_{blender}} . \tag{8}$$

In this study, both the RC hopper and the TP hopper function on the same fundamental concept. Modeled within this project, these hoppers consist of a conical base and a cylindrical top section. The description of the hopper model provided below will determine both the resulting height and mass flow rate. Under stable conditions, the mass flow across all units remains consistent. Therefore, both hoppers will function under similar running circumstances.

The system's dynamics are governed by the mass balance equation (Chindruș *et al.*, 2022), defined as the discrepancy between the inlet mass flow rate from the blender $\left(\dot{m}_{in}\right)$ and the outlet mass flow rate $\left(\dot{m}_{out}\right)$:

$$\rho_b \frac{dV}{dt} = \dot{m}_{in} - \dot{m}_{out} , \tag{9}$$

where ρ_b denotes the density at the outlet of the hopper and V represents the volume of material in the hopper.

The roller compaction process is central to converting a powder blend into a ribbon shape through the utilization of counter-rotating rolls for material compression. Initially, as particles are introduced to the rolls, they are situated within the slip region of the process (Rogers *et al.*, 2013). The nip region represents the area where the rolls are in closest proximity. Subsequently, the release region marks the point at which the ribbon is extricated from the rolls and propelled onward. This process is intricate due to its reliance on numerous parameters and adherence to precise operational criteria.

In this model, a critical factor is the nip angle, which is the angular position $(\theta = \alpha)$, where the material goes from slip to non-slip properties. It is based on material-related characteristics and the subsequent equation is employed for its determination:

$$\frac{4\left(\frac{\pi}{2}-\alpha-\nu\right)\tan\delta_E}{\cot(B-\mu)-\cot(B+\mu)} = \frac{K\left(2\cos\alpha-1-\frac{h_0}{R}\right)\tan\alpha}{\cos\alpha}. \tag{10}$$

Here ν is a variable derived in relation to the effective angle of friction (δ_E) and the angle of wall friction. Additionally, K denotes the compressibility factor, h_0 represents half of the roll gap width and R indicates the radius of the roll. The variables B and μ are determined as illustrated:

$$\begin{aligned} B &= \frac{\alpha+\mu+\frac{\pi}{2}}{2}, \\ \mu &= \frac{\pi}{4}-\frac{\delta_E}{2}. \end{aligned} \tag{11}$$

Within the nip region, the compression behavior can be assessed using an empirical model, $\sigma = C_1\rho^K$, where σ denotes the material stress and ρ signifies the compact density, while C_1 stands for pre-exponential coefficient of material compression.

The roller compactor model described in Eq. (12) was determined utilizing Johanson's model (Johanson, 1965) and the mass balance equation (Chindruş *et al.*, 2022):

$$\begin{aligned} &\int_0^{\theta_{in}} \rho(\theta)\cos\theta d\theta = \underbrace{\int_0^{a} \rho(\theta)\cos\theta d\theta}_{nip\ region} + \underbrace{\int_a^{\theta_{in}} \rho(\theta)\cos\theta d\theta}_{slip\ region} = \\ &= \rho_{exit}\left(\frac{h_0}{R}\right)\left\{\frac{2\left(1+\frac{h_0}{R}\right)}{\sqrt{\frac{h_0}{R}\left(2+\frac{h_0}{R}\right)}}\tan^{-1}\left[\sqrt{1+\frac{2R}{h_0}}\tan\frac{\alpha}{2}\right]-\alpha\right\}+\rho_{in}(\cos\nu-\sin\alpha). \end{aligned} \tag{12}$$

Here, (ρ_{exit}) is the compact density at the exit point, (ρ_{in}) is the inlet density, θ_{in} represents a variable equal to $\pi/2-\nu$ and $\rho(\theta)$ denotes the

density profile, relative to angular position θ. The outlet mass flow rate can be computed, $\dot{m}_{out} = RWhW\rho_{exist}$, where W denotes the roll width and $h = 2h_0$.

The process of compression involves consolidating powder mixtures to produce tablets. Evaluation of tableting procedures includes the examination of multiple factors such as weight consistency, active ingredient content, uniformity of content, and physical characteristics including dissolution behavior, hardness, and friability (Rogers *et al.*, 2013). In this particular investigation, the central objective of developing the tableting process model is to ascertain both tablet hardness and the outflow rate of tablets. To address this aim, the pre-compression $\left(C\_P_{pre}\right)$ and main compression $\left(C\_P_{main}\right)$ pressures are determined using the Kawakita equation (Singh *et al.*, 2012):

$$\begin{aligned} C\_P_{pre} &= \frac{V_0 - V_{pre}}{b_{pre}\left(V_0\left(\varepsilon_0 - 1\right) + V_{pre}\right)} \\ C\_P_{main} &= \frac{V_{pre} - V_{tablet}}{b_{main}\left(V_{pre}\left(\varepsilon_{main} - 1\right) + V_{tablet}\right)} \end{aligned}, \tag{13}$$

where b_{pre} and b_{main} are material dependent parameters. Following this, the necessary volumes (V_{tablet} for the volume of the tablet, pre-compression volume V_{pre} and the feed volume V_0) are defined in subsequent equations (Chindruș *et al.*, 2023):

$$\begin{aligned} V_{tablet} &= L_{tablet} A_{tablet}, \\ V_{pre} &= L_{pre} A_{tablet}, \\ V_0 &= L_{depth} A_{tablet}, \end{aligned} \tag{14}$$

where A_{tablet} indicates the tablet area and L_{tablet}, L_{pre} and L_{depth} represent the tablet height, powder height in the die, and compressed powder height in the die, respectively. It is relevant to mention that, in this process model, pre-compression and main compression forces are obtained by multiplying the associated pressures by 10^6.

Lastly, tablet hardness is determined according to:

$$H_{tablet} = H_{\max}\left(1 - e^{\frac{(1-\varepsilon_0)V_0}{V_{tablet}} - \rho_{rc} + \log\frac{1-(1-\varepsilon_0)V_0}{(14-\rho_{rc})V_{tablet}}}\right), \tag{15}$$

where maximum tablet hardness $(H_{\max})$ and critical relative density (ρ_{rc}) are known variables.

Regarding the mass flow out of the tablet, this is calculated as the product of the production rate (R_{tablet}) and the mass of a single tablet (m_{tablet}), $\dot{m} = R_{tablet} m_{tablet}$, where $(R_{tablet} = T_{turret} n_{die} 60)$, takes into account the turret speed (T_{turret}) and the number of dies on the turret (n_{die}).

3. Control algorithms' design

One of the system design problems is the control of the developed system (Athans and Falb, 2013). LQR and MPC are two iconic control strategies in the implementation of control systems. Both methods approach optimal control by minimizing a performance index and are commonly used in process industries, such as energy management (Gatsis *et al.*, 2014), power electronics (Vazquez *et al.*, 2014), automotive (Sam *et al.*, 2000), chemical industry (Di Cairano, 2012).

In pharmaceutical manufacturing, the Linear Quadratic Regulator (LQR) and Model Predictive Control (MPC) are essential for optimizing production processes. The LQR method, designed to provide optimal stability and robustness, is used to centrally control key process units in tablet production, such as in the dry granulation process. By minimizing a cost function that balances system performance and control effort, LQR ensures precise control over variables like pressure and temperature, enhancing product consistency, reducing waste, and improving efficiency (Lee *et al.*, 2015).

Rather, Model Predictive Control (MPC) employs a dynamic model to predict future system behavior and optimize control actions. This approach is particularly advantageous for managing complex, multi-variable processes typical of pharmaceutical manufacturing (Jelsch *et al.*, 2021). MPC anticipates deviations and adjusts control inputs proactively, maintaining product quality and regulatory compliance. Its ability to handle input and output constraints makes MPC ideal for keeping the production process within safe and efficient operating limits, thereby ensuring high-quality outcomes in a more dynamic environment.

3.1. Linear Quadratic Regulator (LQR)

Expanding on the discussed model, this section presents a comprehensive control strategy for the entire process employing an LQR controller suited to the specifications of the described system. Unlike the conventional Proportional-Integral-Derivative (PID) controller, this control algorithm accommodates multiple feedback variables, which are inherent among the state variables. Consequently, this approach provides richer

information about the system at any given time, leading to a more robust control algorithm. This method is rooted in classical design techniques aimed at optimizing processes by minimizing a quadratic cost function (Anderson and Moore, 2007). Derived from this fundamental concept, various approaches can be explored, including Linear Quadratic Integral control (LQI) or Linear Quadratic Gaussian regulator (LQG).

The implementation of a control structure with state feedback relies on a mathematical model, typically represented in matrix form as a state space model:

$$\begin{aligned} x_d[t+1] &= A_d x_d[t] + B_d u_d[t] \\ y_d[t] &= C_d x_d[t] + D_d u_d[t] \end{aligned}, \tag{16}$$

for a discrete-time representation, where A_d and B_d are the discretized matrices of the system that are known, while x_d, u_d and y_d represent the state, control, and output vectors of the system.

To determine the optimal control vector expressed as follows:

$$u_d[t] = -K_d x_d[t], \tag{17}$$

where K_d is the state variable feedback gain, it is important to minimize the J_d cost function, in order to determine the optimal control inputs, while optimizing the state variables at the same time:

$$J_d = \sum_{t=0}^{\infty} \{x_d^T[t] Q_d x_d[t] + u_d^T[t] R_d u_d[t] + 2x_d^T[t] N_d u_d[t]\}, \tag{18}$$

where the weighting parameters, Q_d and N_d, represent semi-positive definite symmetric matrices, and R_d is a positive definite symmetric matrix. These are required to optimally control each state of the system using as little effort as possible according to the performance index described above. Basically, the choice of weight matrices Q_d and R_d determines the closed-loop performance.

The final step in calculating the optimal control vector is to determine the optimal feedback gain (Bao-Cang, 2010):

$$K_d = \left(B_d^T S_d B_d + R_d\right)^{-1} \left(B_d^T S_d A_d + N_d^T\right), \tag{19}$$

where S_d is the solution of the corresponding discrete algebraic Riccati equation (Anderson and Moore, 2007):

$$A_d^T S_d A_d - S_d - \left(A_d^T S_d B_d + N_d\right)\left(B_d^T S_d B_d + R_d\right)^{-1} \left(B_d^T S_d A_d + N_d^T\right) + Q_d = 0. \tag{20}$$

3.2. Linear Quadratic Integral (LQI) regulator

When a non-constant reference must be tracked, it is necessary to introduce an integrator in terms of the integral of the error in the control loop. The Linear Quadratic Regulator with Integral action, whose design is based on the formulation of LQR, can make the steady-state error equal to zero. The difference between them consists in the introduction of an integrator for the latter. Integral control is added to the LQ problem to reduce the steady-state error for a desired reference and to increase the performances of the control system (Wang, 2009). An important feature of controllers with integral feedback is their ability to handle constant disturbances.

The incorporation of integral action involves the addition of an extra state (x_i) to the state vector (x_d), signifying the integral of the error between the desired output r and the actual output y_d. Therefore, the augmented state vector can be expressed as:

$$x_e = \begin{bmatrix} x_d \\ x_i \end{bmatrix}, \tag{21}$$

where $x_i[t+1] = x_i[t] + T_s\left(r[t] - y_d[t]\right)$, with sampling time T_s.

The optimal control law using integrator in the context of LQ problem is described as:

$$u_i = -K_i x_e, \tag{22}$$

where K_i is the optimal gain matrix, calculated from Eqs. (19) and (20).

3.3. State estimation – Luenberger Observer

Usually, in the implementation of any type of controller, when the full state variable $x_d[t]$ at time t is not accessible to measurements, the use of an observer is required. The approach of Luenberger observer (Antsaklis and Michel, 2006) is to model the current system with a correction term, based on the measured output y_d and its estimate $\hat{y}_d$.

Under observability assumptions on the pair (A_d, C_d) of the discretized system from Eq. (16), a full-order observer can be described as (Rawlings *et al.*, 2017):

$$\begin{aligned} \dot{\hat{x}}_d &= A_d \hat{x}_d + B_d u_d + K_L \left(y_d - \hat{y}_d \right) \\ \hat{y}_d &= C_d \hat{x}_d \end{aligned}, \tag{23}$$

where K_L is the constant observer gain matrix. A classical technique to design the observer is the pole assignment. Depending on the choice of gain matrix K_L, the system $\left(A_d, C_d \right)$ may have different states. If matrix K_L can be chosen to place the eigenvalues of $A_d - K_L C_d$ at arbitrary locations in plane, then the system will be completely observable.

The purpose of this observer is to produce an estimate of the true state $x_d[t]$. Considering the definition of the estimation error:

$$e_d(t) = x_d(t) - \hat{x}_d(t), \tag{24}$$

the constructed observer gives the following dynamics for the estimation error:

$$\dot{e}_d(t) = \dot{x}_d(t) - \dot{\hat{x}}_d(t) = \left(A_d - K_L C_d \right) e_d(t). \tag{25}$$

4. Experimental results

The performance evaluation of the proposed methods in this study was conducted using the simulation and testing environment, Matlab/Simulink. Both strategies were implemented and tested on a common benchmark simulator to ensure a fair comparison of their results. The system under consideration is characterized as an 8×8 input-output system (see Fig. 3), with nominal values and associated constraints detailed in Table 2 and Table 3 (Chindruș *et al.*, 2022).

To assess the effectiveness of both controllers, the control limits for the controlled variables were determined as $+/-2\%$ of their reference values.

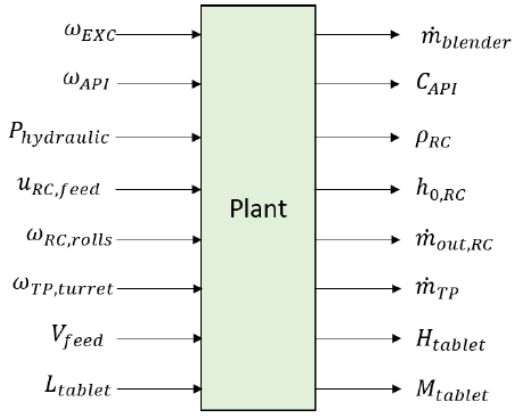

Fig. 3 – Schematic representation of the plant (Chindruș *et al.*, 2023).

Table 2
Nominal values and constraints of the input variables (Malevez and Copoț, 2021)

Input variable	Nominal	LB	UB	unit
Screw speed Excipient (ω_{Exc})	207.6	0	240	rpm
Screw speed API (ω_{API})	37.4	0	240	rpm
Velocity rolls $(\omega_{RC,rolls})$	5	1	10	rpm
Feed speed (u_d)	2.017	1	5	cm/s
Hydraulic pressure $(P_{hydraulic})$	1	1	10	MPa
Height tablet (L_{tablet})	4	3.8	5	mm
Feed volume (V_{feed})	0.96	0.9	1.1	cm^3
Turret speed $(\omega_{TP,turret})$	45	40	50	rpm

In what follows, the LQI results are compared with the ones obtained with the MPC method in a setpoint tracking experiment. Furthermore, in the LQI case, at time $T = 1400s$, a step disturbance was introduced to test whether it is rejected by the system.

Table 3
Nominal values and constraints of the output variables (Malevez and Copoț, 2021)

Output variable	Nominal	LB	UB	unit
Mass flowrate $(\dot{m}_{blender})$	20	17	23	kg/h
Concentration API (C_{API})	0.15	0.10	0.20	-
Density outlet (ρ_{RC})	1.057	0.8	1.2	g/cm^3
Throughput $(\dot{m}_{out,RC})$	20	17	23	kg/h
Roller gap $(h_{0,RC})$	1.6	1	5	mm
Hardness (H_{tablet})	5.433	4	6	MPa
Mass tablet (M_{tablet})	0.4566	0.44	0.47	g
Tablet rate $(\dot{m}_{TP})$	20	17	23	kg/h

The performance of LQR control algorithm depends on the tuning method of the design parameters (Q_d, R_d) from Eq. (18). As the LQI constitutes a full-state feedback controller, an observer becomes essential to furnish the system states based on the accessible measurements. Furthermore, both the

controller and observer entail multiple parameters that necessitate determination. In Matlab, the parameters essential for designing the LQI controller are identified through the *lqi* function, structured as follows:

$$\left[K_d, S_d, e_d\right] = lqi\left(SYS, Q_d, R_d, N_d\right), \tag{26}$$

where e_d are the closed-loop poles.

Before adding the integrators, the matrix Q_d had dimension 251×251, the same as the matrix (A_d) associated with the system states (x_d). After inserting the integrators associated to each system output, the matrix Q_d has size 259×259. The Q_d and R_d matrices used to calculate the optimal gain K_d are expressed as follows:

$$Q_d = \begin{pmatrix} \mathrm{O}_{35\times 35} & \mathrm{O}_{35\times 8} & \mathrm{O}_{35\times 208} & \mathrm{O}_{35\times 8} \\ \mathrm{O}_{8\times 35} & Q_o & \mathrm{O}_{8\times 208} & \mathrm{O}_{8\times 8} \\ \mathrm{O}_{208\times 35} & \mathrm{O}_{208\times 8} & \mathrm{O}_{208\times 208} & \mathrm{O}_{208\times 8} \\ \mathrm{O}_{8\times 35} & \mathrm{O}_{8\times 8} & \mathrm{O}_{8\times 208} & Q_i \end{pmatrix}, \tag{27}$$

$$R_d = \mathrm{I}_8$$

where $\mathrm{O}_{m\times n}$ is the zero matrix and I_8 is the identity matrix of size 8. Q_o and Q_i, described in Eq. (28), are matrices whose diagonals contain the values of the weights associated with the outputs and integrators, respectively.

$$Q_o = \begin{pmatrix} 10^2 & 0 & 0 & 0 & 0 & 0 & 0 & 0 \\ 0 & 10^5 & 0 & 0 & 0 & 0 & 0 & 0 \\ 0 & 0 & 10^2 & 0 & 0 & 0 & 0 & 0 \\ 0 & 0 & 0 & 10^2 & 0 & 0 & 0 & 0 \\ 0 & 0 & 0 & 0 & 1 & 0 & 0 & 0 \\ 0 & 0 & 0 & 0 & 0 & 10^2 & 0 & 0 \\ 0 & 0 & 0 & 0 & 0 & 0 & 10^2 & 0 \\ 0 & 0 & 0 & 0 & 0 & 0 & 0 & 10^2 \end{pmatrix}, Q_i = \begin{pmatrix} 10^3 & 0 & 0 & 0 & 0 & 0 & 0 & 0 \\ 0 & 10^8 & 0 & 0 & 0 & 0 & 0 & 0 \\ 0 & 0 & 10^3 & 0 & 0 & 0 & 0 & 0 \\ 0 & 0 & 0 & 10^3 & 0 & 0 & 0 & 0 \\ 0 & 0 & 0 & 0 & 1 & 0 & 0 & 0 \\ 0 & 0 & 0 & 0 & 0 & 10^3 & 0 & 0 \\ 0 & 0 & 0 & 0 & 0 & 0 & 10^3 & 0 \\ 0 & 0 & 0 & 0 & 0 & 0 & 0 & 10^3 \end{pmatrix} \cdot \tag{28}$$

The numerical values for the matrices described in Eqs. (27) and (28) were computed based on heuristics. The performance of the controller is influenced by the weighting matrices, which were determined through a heuristic approach. This method involves iterative testing and tuning to achieve optimal performance. By adjusting these matrices, we were able to balance the trade-offs between control effort and system stability, ensuring that the controller effectively manages disturbances and tracks reference signals within the desired limits.

In (Copoț *et al*., 2022), starting from the same plant, a control strategy based on the MPC architecture is developed. The approach involves decomposing the overall model into distinct subsystems that are dynamically interconnected via their inputs and are subject to specific input constraints. Each subsystem is analyzed in isolation, with neighboring elements being identified, and cost functions are formulated based on predicted future output trajectories. By applying the superposition principle, which is valid for linear systems, the anticipated system response is computed. This response is derived as the cumulative result of the projected future scenarios and the corresponding optimization impacts:

$$Y_i = \overline{Y}_i + Y_i^{opt}, \tag{29}$$

where $\overline{Y}_i$ is the basic future scenario, Y_i^{opt} is the effect of the optimizing future control actions and i referred to the associated subsystem.

Both the Linear Quadratic Regulator and Model Predictive Control represent optimal control techniques, each employing distinct methodologies to ascertain optimization costs. A fundamental discrepancy between the two lies in their approach to optimization computation. While MPC necessitates solving optimization problems iteratively at each time step, LQR involves a singular optimization computation. Consequently, MPC mandates real-time optimization, whereas LQR involves a one-time computation of the gain matrix K_d.

In this study, the performance of the Linear Quadratic Regulator with Integral action is evaluated in comparison to the Model Predictive Control strategy proposed by (Copoț *et al.*, 2022). The effectiveness of the designed LQI controller is demonstrated in achieving two primary objectives: disturbance rejection and reference tracking. Notably, the time interval $[0,50]s$ denotes the duration until the system stabilizes and attains normal operation, rendering variations during this period inconsequential to the strategy's performance.

Fig. 4 and Fig. 5 showcase the closed-loop response for the mass flow rate at the outlet of the blender unit for both methodologies, which should align with the mass flow rate at the roller compactor (Fig. 6 and Fig. 7). Therefore, maintaining identical setpoints for both mass flow rates at both units is imperative.

It is observed that, in terms of stability, the LQI method provides improved results, compared to MPC, which is more obvious in the case of the concentration of API (Fig. 8, Fig. 9) and outlet mass flow rate RC (Fig. 6, Fig. 7). Concerning the hardness of the tablet (Fig. 10 and Fig. 11), the system output in case of LQI remains within the defined operating range.

In addition, in the quadratic linear control approach, a step disturbance was added at time $T = 1400s$. This allowed the analysis of the flexibility of the system in the presence on inherent process variability or external disturbances.

In the corresponding subplots, highlighted on the figures on the right side, it can be observed that the system successfully rejects this disturbance in a very short time. It is also shown how the change of reference at time $T = 500s$ for mass flow rate at the blender, mass flow rate RC and hardness influences the other outputs.

Figures 12 and 13 illustrate the performance obtained in the case of a constant reference, and how the step changes made for tablet hardness (at time $T = 500s$ and $T = 1100s$) and the introduced disturbance affect tablet mass output.

5. Conclusions

The field of cyber-physical systems is continuously expanding in a wide range of domains, such as energy and industrial automation, critical infrastructure, transportation, or health and biomedical. This type of complex systems offers new operating capabilities and is a much more efficient and secure way for production and development. In this paper, a comparative analysis of two emblematic control strategies, LQR and MPC, has been made in a continuous production simulator of solid oral tablets. The results obtained using the linear quadratic method illustrate improved performance, compared to predictive control.

The superior performance of the LQI method over MPC can be attributed to several key factors. Firstly, the LQI method optimizes a cost function that directly balances control performance and effort, allowing for rapid and stable responses to disturbances. This optimization is particularly effective in the dry granulation process of tablet production, where maintaining precise control over critical parameters such as pressure and material flow is essential. Additionally, the LQI method's straightforward control structure ensures robust and reliable performance, making it highly effective in scenarios with well-understood system dynamics.

In contrast, while MPC is highly effective in managing complex, multi-variable processes with its predictive capabilities, it often requires more computational resources and can be slower in responding to sudden disturbances. The need for an accurate process model and the inherent computational complexity can sometimes limit MPC's responsiveness. Thus, in the context of our study, the LQI method demonstrated superior performance by providing quicker disturbance rejection and more stable reference tracking, thereby ensuring higher efficiency and consistency in the production process.

Continuous manufacturing represents a promising frontier in pharmaceutical production with high potential for exploitation, and reform is needed because pharmaceutical production no longer satisfies the demands of the market and people's needs. Future research will concentrate on devising an integrated control strategy specifically for pharmaceutical tablet manufacturing

systems. This strategy will address dynamic challenges such as time-varying delays and data-packet losses, aiming the way for enhanced efficiency and productivity.

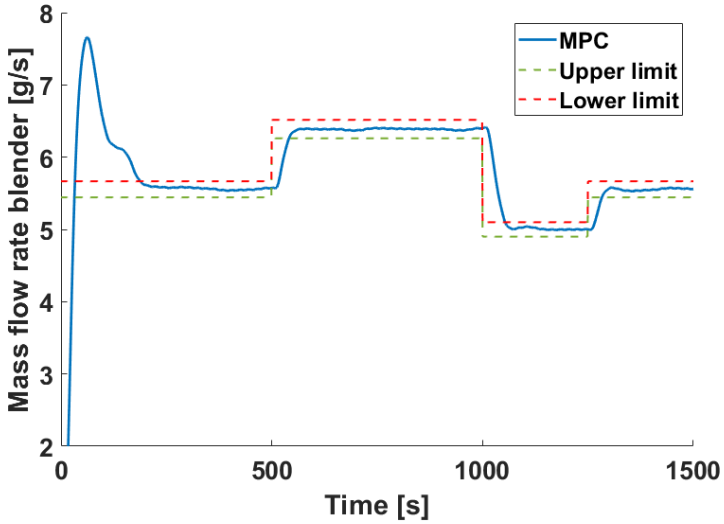

Fig. 4 – MPC performance for mass flow rate of the blender.

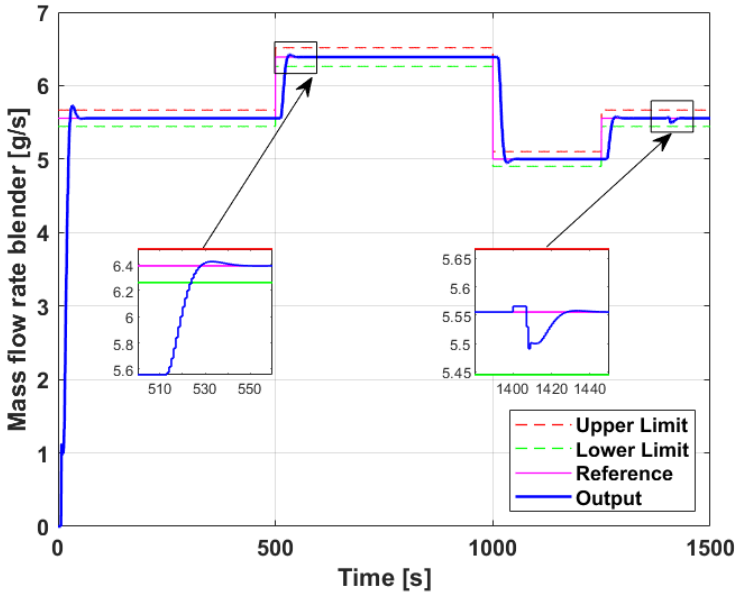

Fig. 5 − LQI performance for mass flow rate of the blender.

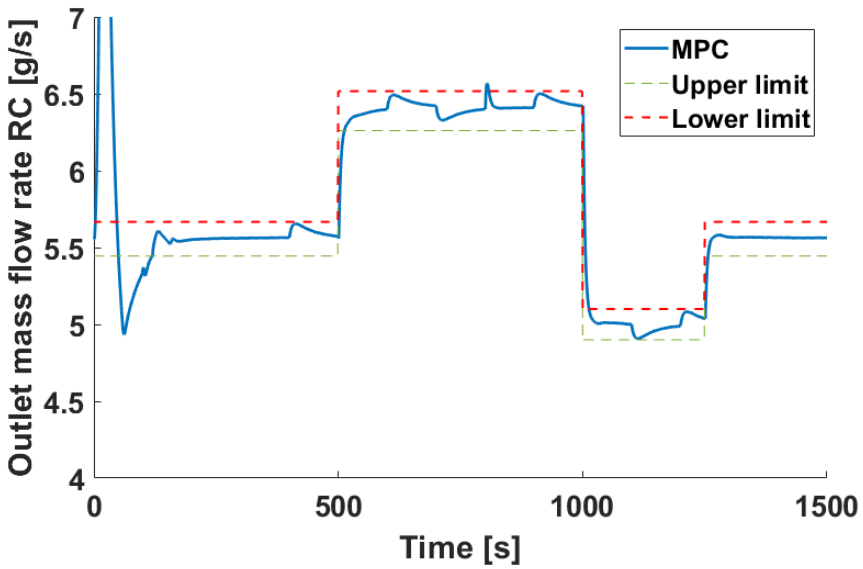

Fig. 6 − MPC performance for outlet mass flow rate RC.

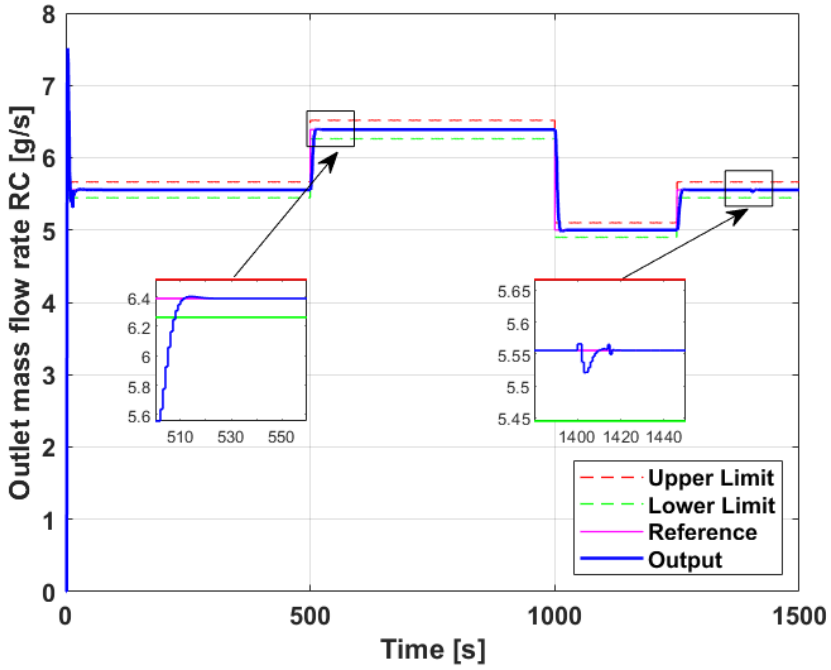

Fig. 7 − LQI performance for outlet mass flow rate RC.

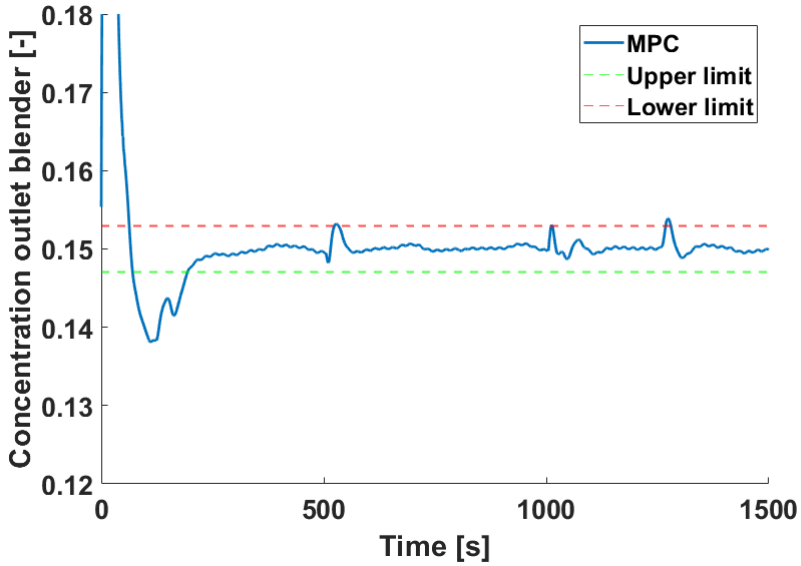

Fig. 8 − MPC performance for the concentration of API.

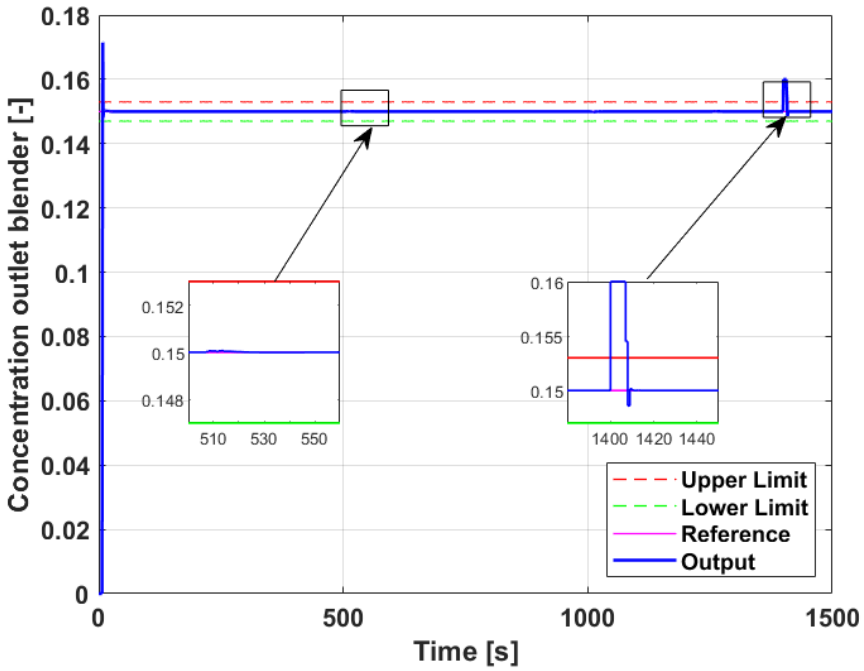

Fig. 9 − LQI performance for the concentration of API.

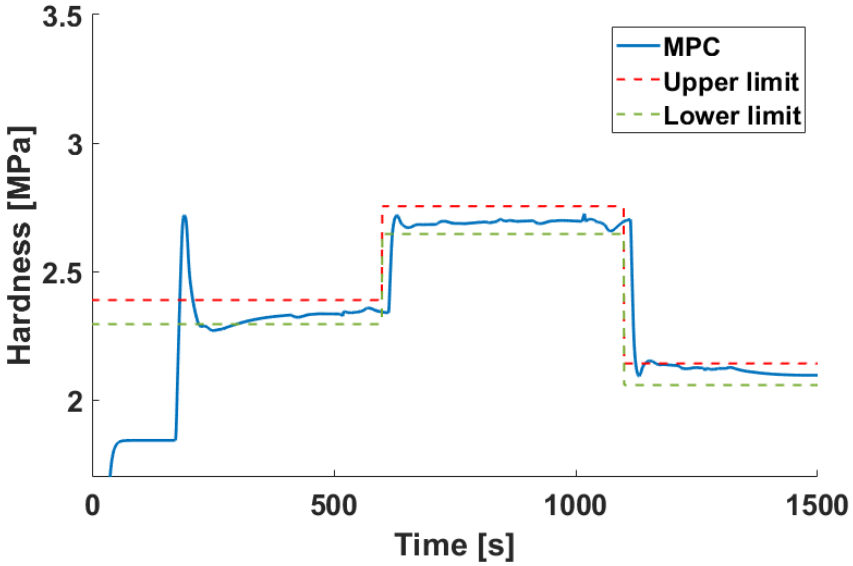

Fig. 10 − MPC performance for tablet hardness.

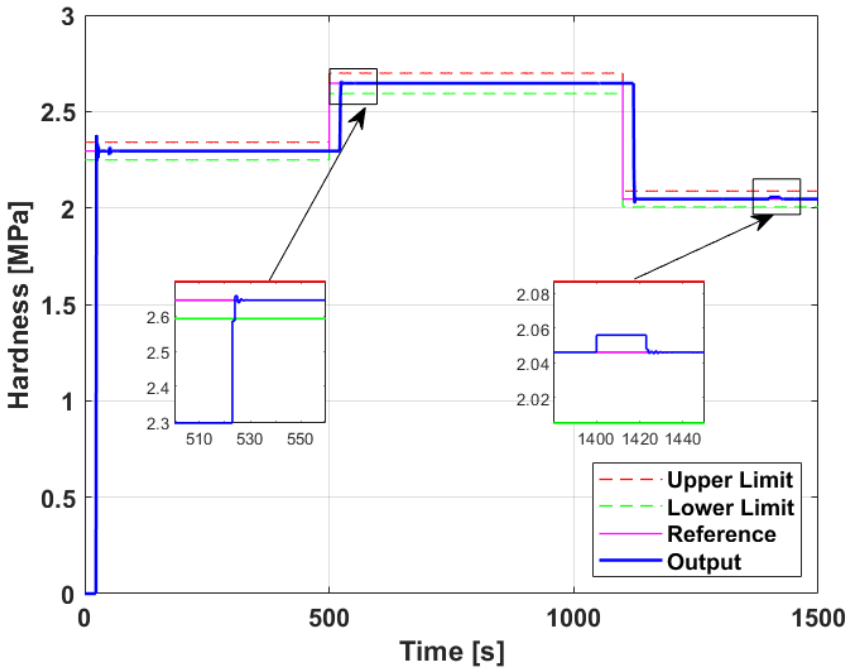

Fig. 11 − LQI performance for tablet hardness.

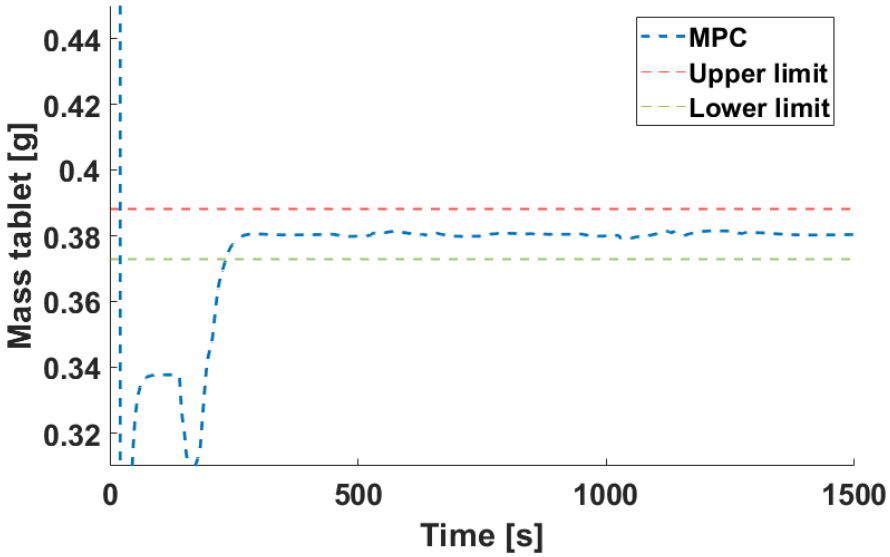

Fig. 12 − MPC performance for the mass of the tablet.

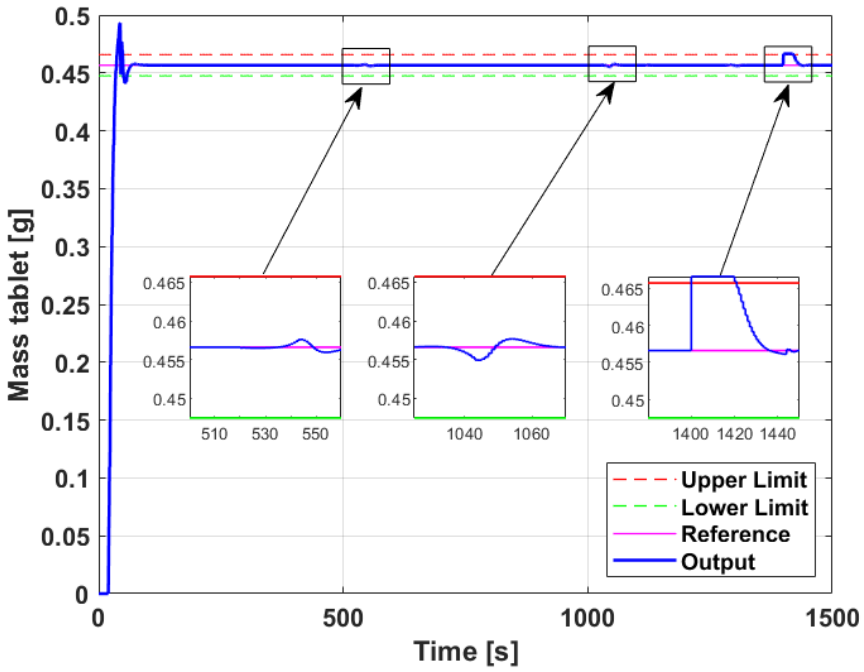

Fig. 13− LQI performance for the mass of the tablet.

REFERENCES

Anderson B.D., Moore J.B., *Optimal control: linear quadratic methods*, Courier Corporation, 2007.

Antsaklis P.J., Michel A.N., *State feedback and state observers*, Linear Systems, pp. 321–382, 2006.

Athans M., Falb P.L., *Optimal control: an introduction to the theory and its applications*, Courier Corporation, 2013.

Bao-Cang D., *Modern predictive control*, CRC press, 2010.

Bhalode P., Ierapetritou M., *Discrete element modeling for continuous powder feeding operation: Calibration and system analysis*, International Journal of Pharmaceutics, 585:119427, 2020.

Bhowmik D., Duraivel S., AN R., Kumar K.S., *Tablet manufacturing process and defects of tablets*, Elixir Pharmacy, 70:24368-74, 2014.

Caylar P.L., Noterdaeme O., Naik K., *Digital in industry: From buzzword to value creation*, Mckinsey Company, Digit. Mckinsey 2, no. 1, 2016.

Chindruș A., Copoț D., Căruntu C.F., *Continuous Manufacturing using Linear Quadratic Regulator in the Context of Cyber-Physical Systems,* 26th International Conference on System Theory, Control and Computing, pp. 231-236, IEEE, 2022.

Chindruș A., Copoț D., Căruntu C.F., *Predictive control strategy for Continuous Production Systems: A comparative study with classical control approaches using simulation-based analysis*, Processes, 11(4), 1258, 2023.

Copoț D., Căruntu C.F., Portier C., De Keyser R., Ionescu C.M., *An open source benchmark simulator for sustainable and flexible pharmaceutical manufacturing*, 28th International Conference on Emerging Technologies and Factory Automation, Sinaia, Romania, 2023.

Deka L., Khan S.M., Chowdhury M., Ayres N., *Transportation Cyber-Physical System and its importance for future mobility*, Elsevier, Pages 1-20, 2018.

Dey N., Ashour A.S., Shi F., Fong S.J., Tavares J.M.R.S., *Medical cyber-physical systems: A survey*, J Med Syst 42, 74, 2018.

Di Cairano S., *An industry perspective on MPC in large volumes applications: Potential Benefits and Open Challenges*, IFAC Proceedings Volumes, 45(17):52-9, 2012.

Do Q., Martini B., Choo K.-K.R., *Cyber-physical systems information gathering: A smart home case study, Computer Networks*, Volume 138, Pages 1-12, 2018.

Escotet Espinoza M., *Phenomenological and residence time distribution models for unit operations in a continuous pharmaceutical manufacturing process*, Ph.D. dissertation, Rutgers University-School of Graduate Studies, 2018.

Gatsis K., Ribeiro A., Pappas G.J., *Optimal Power Management in Wireless Control Systems*, in IEEE Transactions on Automatic Control, vol. 59, no. 6, pp. 1495-1510, 2014.

Haas N.T., Ierapetritou M., Singh R., *Advanced model predictive feedforward/feedback control of a tablet press*, Journal of Pharmaceutical Innovation, vol. 12, no. 2, pp. 110–123, 2017.

Haunreiter K. J., *200th anniversary of the paper machine*, Tappi journal 80(10), p.89, 1997.

Jazdi N., *Cyber physical systems in the context of Industry 4.0*, IEEE international conference on automation, quality and testing, robotics, pp. 1-4, IEEE, 2014.

Jelsch M., Roggo Y., Kleinebudde P., Krumme M., *Model predictive control in pharmaceutical continuous manufacturing: A review from a user's perspective*, European Journal of Pharmaceutics and Biopharmaceutics, vol. 159, pp. 137–142, 2021.

Jha A.V., Appasani B., Ghazali A.N., Pattanayak P., Gurjar D.S., Kabalci E., Mohanta D.K., *Smart grid cyber-physical systems: communication technologies, standards and challenges*, Wireless Netw 27, 2595–2613, 2021.

Johanson J.R., *A Rolling Theory for Granular Solids*, Journal of Applied Mechanics, vol. 32, no. 4, pp. 842–848, 12, 1965.

Lee S.L., O'Connor T.F., Yang X., Cruz C.N., Chatterjee S., Madurawe R.D., Moore C., Yu L.X., Woodcock J., *Modernizing pharmaceutical manufacturing: from batch to continuous production*, Journal of Pharmaceutical Innovation, 10(3):191-9, 2015.

Malevez D., Copot D., *From batch to continuous tablet manufacturing: A control perspective*, IFAC-PapersOnLine, 54(15):562-7, 2021.

Rawlings J., Mayne D., Diehl M., *Model Predictive Control: Theory, Computation, and Design 2nd Edition*, Nob Hill Publishing, 2017.

Rogers A.J., Hashemi A., Ierapetritou M.G., *Modeling of particulate processes for the continuous manufacture of solid-based pharmaceutical dosage forms*, Processes, 1(2):67-127, 2013.

Sam Y.M., Ghani M.R., Ahmad N., *LQR controller for active car suspension*, TENCON Proceedings, Intelligent Systems and Technologies for the New Millennium (Cat. No. 00CH37119), Vol. 1, pp. 441-444, IEEE, 2000.

Sen M., Singh R., Vanarase A., John J., Ramachandran R., *Multi-dimensional population balance modeling and experimental validation of continuous powder mixing processes*, Chemical engineering science, 80:349-60, 2012.

Singh R., Ierapetritou M., Ramachandran R., *An engineering study on the enhanced control and operation of continuous manufacturing of pharmaceutical tablets via roller compaction*, International journal of pharmaceutics, 438(1-2):307-26, 2012.

Tao F., Cheng J., Qi Q., *An Industrial Internet-of-Things Hub Toward Smart Manufacturing Based on Cyber-Physical System*, in IEEE Transactions on Industrial Informatics, vol. 14, no. 5, pp. 2271-2280, 2018.

Vazquez S., Leon J.I., Franquelo L.G., Rodriguez J., Young H.A., Marquez A., Zanchetta P., *Model predictive control: A review of its applications in power electronics*, IEEE industrial electronics magazine, 8(1):16-31, 2014.

Wang L. *Model predictive control system design and implementation using MATLAB*, Springer Science & Business Media, 2009.

Wang Z., Escotet-Espinoza M.S., Ierapetritou M., *Process Analysis and optimization of continuous pharmaceutical manufacturing using flowsheet models*, Computers and Chemical Engineering 107, 77–91, 2017.

Yu Y., *Theoretical modelling and experimental investigation of the performance of screw feeders*, Ph.D. dissertation, University of Wollongong, 1997.

COMPARAREA REGULATORULUI LINIAR PĂTRATIC ȘI A ALGORITMILOR BAZAȚI PE CONTROLUL PREDICTIV ÎN PRODUCȚIA CONTINUĂ

(Rezumat)

Integrarea Industriei 4.0 în procesele de fabricație necesită automatizarea operațiunilor complexe, la scară largă, în cadrul sistemelor cibernetico-fizice (CPS). Producția farmaceutică, în special, necesită o tranziție de la procesarea tradițională pe loturi la producția continuă pentru a realiza o integrare fără probleme cu CPS-urile. Această lucrare explorează comparația dintre două strategii de control pentru producția de tablete farmaceutice: metoda regulatorului liniar pătratic (LQR) și un algoritm consacrat de control predictiv bazat pe model (MPC). Metoda LQR se concentrează pe asigurarea unei stabilități și a unei robusteți optime pentru operațiunile fabricii, în special prin gestionarea centralizată a unităților de proces cheie în procesul de granulare uscată. Un model detaliat al instalației este utilizat pentru a testa performanța regulatorului LQR, rezultatele fiind comparate cu cele obținute cu ajutorul algoritmului MPC.